Journal of Power Sources 251 (2014) 357–362

Contents lists available at ScienceDirect

Journal of Power Sources

journal homepage: www.elsevier.com/locate/jpowsour

Cerium and niobium doped $SrCoO_{3-\delta}$ as a potential cathode for intermediate temperature solid oxide fuel cells

Shouguo Huang*, Shuangjiu Feng, Qiliang Lu, Yide Li, Hong Wang, Chunchang Wang*

Laboratory of Dielectric Functional Materials, School of Physics and Materials Science, Anhui University, Hefei 230601, PR China

HIGHLIGHTS

- SCCN exhibits sufficiently high electronic conductivity and excellent chemical compatibility with SDC electrolyte.
- Highly charged Ce^{4+} and Nb^{5+} successfully stabilize the perovskite structure.
- The ASRs of the SCCN–SDC cathode are 0.027 and 0.049 Ω cm^2 at 700 and 650 °C, respectively.
- SCCN is promising as a cathode material for ITSOFCs.

ARTICLE INFO

Article history:
Received 22 July 2013
Received in revised form
19 November 2013
Accepted 28 November 2013
Available online 7 December 2013

Keywords:
Solid oxide fuel cell
Cathode
Electrochemical properties
Oxygen reduction reaction
Perovskite

ABSTRACT

$Sr_{0.9}Ce_{0.1}Co_{0.9}Nb_{0.1}O_{3-\delta}$ (SCCN) has been synthesized using solid state reaction, and investigated as a new cathode material for intermediate temperature solid oxide fuel cells (ITSOFCs). SCCN material exhibits sufficiently high electronic conductivity and excellent chemical compatibility with SDC electrolyte. Highly charged Ce^{4+} and Nb^{5+} successfully stabilize the perovskite structure to avoid order–disorder phase transition. The electrical conductivity reaches a high value of 516 S cm^{-1} at 300 °C in air. The area specific resistances of the SCCN-50 wt.% $Ce_{0.8}Sm_{0.2}O_{1.9}$ (SDC) cathode are as low as 0.027, 0.049, and 0.094 Ω cm^2 at 700, 650, and 600 °C, respectively, with the corresponding peak power densities of 1074, 905, and 589 mW cm^{-2}. A relatively low thermal expansion coefficient of SCCN–SDC is 14.3×10^{-6} K^{-1} in air. All these results imply that SCCN holds tremendous promise as a cathode material for ITSOFCs.

© 2013 Elsevier B.V. All rights reserved.

1. Introduction

Solid oxide fuel cells (SOFCs) offer additional advantages over other conventional energy conversion devices in virtue of high efficiency, fuel flexibility, environmental compatibility, as well as the possibility to recover exhaust heat. The development of robust cathode materials for SOFCs operating at intermediate temperatures (IT, 600–800 °C) has attracted much attention because of the potential to dramatically reduce the cost of the raw materials of SOFCs and the fabrication of ceramic structures [1–5]. However, the area specific resistance between the cathode and electrolyte increases rapidly with reducing the operating temperature [6–8]. Therefore, it is critical to develop cathode materials with low polarization losses and high stability for ITSOFCs.

Cobalt-containing perovskites ($SrCoO_{3-\delta}$), such as $La_{0.6}Sr_{0.4}Co_{0.8}Fe_{0.2}O_3$ (LSCF), $Ba_{0.5}Sr_{0.5}Co_{0.8}Fe_{0.2}O_3$ (BSCF) and $Sm_{0.5}Sr_{0.5}CoO_3$, have been investigated intensively as cathode materials for ITSOFCs and oxygen transport membranes due to the high electronic and oxygen-ion conductivities [9–13]. These $SrCoO_{3-\delta}$-based perovskite oxides showed high catalytic activities for oxygen reduction reaction (ORR) in the application of the cathodes for ITSOFCs. However, $SrCoO_{3-\delta}$-based perovskites exhibit the drawbacks mainly associated with their relatively large thermal expansion coefficients and high reactivities (e.g., readily react with yttria-stabilized zirconia electrolytes), which result in instability of the perovskite cubic structure and delamination of between the cathode and electrolyte.

Partial substitution of the B-site element in $SrCoO_{3-\delta}$ by cations with high valencies may lead to the reduce in the ionic radius discrepancy between A-site and B-site cations so that a lower tolerance factor can be obtained, which, in turn, leads the cubic structure to be stabilized [14–18]. This expectation has been confirmed by recent work, for example, Nagai et al. [19] reported

* Corresponding authors. School of Physics and Materials Science, Anhui University, Hefei 230601, PR China. Tel.: +86 551 63861902; fax: +86 551 65846849.
E-mail addresses: huangsg@ustc.edu (S. Huang), ccwang@ahu.edu.cn (C. Wang).

0378-7753/$ – see front matter © 2013 Elsevier B.V. All rights reserved.
http://dx.doi.org/10.1016/j.jpowsour.2013.11.096

that the Nb-doping can efficiently stabilize the cubic perovskite crystal structure of cobalt-containing oxides due to the relative ease of deforming NbO_6 octahedra in comparison with other fixed valent cations, which was noted for both high oxygen-ion and electronic conductivities at elevated temperatures [20–23]. Furthermore, some studies demonstrated that substitution of high valent Ce cations for the Sr in $SrCoO_{3-\delta}$ lead to a good chemical stability of the structure. Moreover, the stabilized $SrCoO_{3-\delta}$ phase exhibited an acceptable electronic conductivity at 700 °C (~300 S cm^{-1}) [24–30]. These facts encourage us to study the electrochemical and structural features of the $SrCoO_{3-\delta}$ perovskites as a cathode material.

In this work, we present detailed investigation on the cerium and niobium co-doped $SrCoO_{3-\delta}$ ($Sr_{0.9}Ce_{0.1}Co_{0.9}Nb_{0.1}O_{3-\delta}$, SCCN) as a new cathode material for ITSOFCs. The electrochemical performance was characterized by electrochemical impedance technique. The performance of the SCCN cathode for ITSOFCs was evaluated with an anode-supported fuel cell and the *I–V* characteristics were analysed.

2. Experimental

$Sr_{0.9}Ce_{0.1}Co_{0.9}Nb_{0.1}O_{3-\delta}$(SCCN) powder was synthesized using the traditional solid state reaction process using analytical grade of $SrCO_3$, CeO_2, Co_3O_4, and Nb_2O_5 as the raw materials. The composite powders were sufficiently mixed by ball milling for 2 h, and then followed by calcinations at 1000 °C for 10 h and 1100 °C for 10 h with intermediate grinding. $Ce_{0.8}Sm_{0.2}O_{1.9}$ (SDC) powders were synthesized via an oxalate co-precipitation process [31]. The as-prepared powders were calcined at 750 °C for 2 h in air. Dense SDC pellets with diameter of 15.0 mm and thickness of 0.7 mm were prepared by dry-pressing, then sintered at 1400 °C for 4 h. The SCCN slurry with 6 wt.% ethyl cellulose terpineol binder was painted onto both sides of the dense SDC electrolyte pellet, and then fired at 1000 °C for 1 h in air to form symmetrical cells with SCCN|SDC|SCCN configurations for the electrochemical impedance studies. Ag paste was then applied to the cathode as a current collector. The SCCN–SDC cathode slurries were screen-printed onto both sides of the SDC electrolyte pellets, and subsequently sintered in air at 1000 °C for 1 h to form symmetrical cells with SCCN–SDC|SDC|SCCN–SDC configurations.

To make a single cell, the anode-supported half cells were fabricated by a tape-casting and co-fired at 1400 °C for 5 h, which resulted in dense SDC film on the NiO–SDC (60:40 wt.%) substrate [32]. The SCCN (or SCCN–SDC) cathode slurry was then painted on SDC electrolyte films, and sintered at 1000 °C for 1 h in air to form single cells of NiO–SDC|SDC|SCCN (or SCCN–SDC).

The crystal structures of the SCCN powders were identified by X-ray diffraction (XRD, MXP18AHF, MARK, Japan) with CuKα radiation. The microstructures of the cathodes were investigated by scanning electron microscopy (SEM, S-4800, Hitachi). Thermogravimetric (TG) analysis profiles were collected with a NETZSCH 449F3 high-temperature thermoanalyzer apparatus from room temperature (RT) to 1000 °C in air. Thermal expansion coefficient (TEC) was measured in air using a dilatometer (PCY III, Huafeng, China) from RT to 1000 °C with a ramp rate of 3 °C min^{-1}. SCCN bar with the dimensions of 5 mm × 5 mm × 12 mm was sintered at 1100 °C in air for the electrical conductivity test. Electrical conductivity was measured in air by the four-terminal dc technique with a Keithley 2400 multimeter at a temperature range of RT to 800 °C.

The electrochemical impedance spectra (EIS) were measured under open current conditions using an electrochemical workstation (CHI650D, Shanghai Chenhua). A 10 mV AC signal was applied and the frequency was swept from 0.01 Hz to 100 kHz. The single cells were tested in a home-made cell testing system in a temperature range of 600–700 °C with humidified hydrogen (3% H_2O) as the fuel and static air as the oxidant.

3. Results and discussion

Fig. 1a shows the XRD patterns of SCCN powders. As seen that the as-prepared SCCN powders exhibit a well-developed crystallization, and all of the peaks can be well indexed based on the cubic perovskite structure. In order to evaluate the chemical compatibility between SCCN and SDC, the SCCN–SDC (1:1 in weight) mixing powders were fired at 1000 °C for 6 h in air. XRD pattern of the mixture of SCCN–SDC powders was presented in Fig. 1b, from which it can be clearly seen that the peaks belong to SCCN and SDC. No alien reflection peaks were observed, indicating that there is no detectable crystalline reaction between SCCN and SDC, i.e., two compounds are chemically compatible at high temperatures.

For a perovskite oxide ABO_3, its structure stability is controlled by the tolerance factor (t) as shown in Eq. (1).

$$t = \frac{r_A + r_O}{\sqrt{2}(r_B + r_O)} \quad (1)$$

where, r_A is the radius of A cation, r_B the radius of B cation, r_O the radius of O anion. When t lies between 0.77 and 1.10, the perovskite structure is stable. The ideal cubic perovskite structure appears in a few cases for t-values very close to 1. The t value of SCCN is 0.99006 according to the empirical ionic radii: $r(Ce^{4+})$ = 0.114 nm, $r(Sr^{2+})$ = 0.144 nm, $r(Co^{3+})$ = 0.061 nm, $r(Nb^{5+})$ = 0.064 nm, and $r(O^{2-})$ = 0.138 nm at room temperature [20,27,29]. This indicates that the SCCN perovskite may form to a cubic perovskite structure. It was reported that doping with the high valent ions raises the electrostatic repulsion [19,33]. Large electrostatic repulsion between the B-site cations can make the hexagonal phase less stable than the perovskite structure due to the crystal-chemical character. Therefore, highly charged cations destabilize the hexagonal structure, and thus stabilize the perovskite structure.

The oxygen vacancies are not only the charge carriers for oxygen-ion transport through the cathode but also the active sites for oxygen adsorption, dissociation and diffusion. Undoubtedly, a higher oxygen-vacancy concentration and a higher electronic conductivity would be beneficial for reducing the resistance of the ORR. Fig. 2 shows TG measurements of the SCCN material performed in air in the temperature range RT–1000 °C. A significant mass loss of the sample can be observed above 250 °C, which is primarily associated with the loss of lattice oxygen and the formation of oxygen vacancy. No plateau can be observed during the heating process, indicating the absence of oxygen order–disorder transition in the SCCN perovskite. Up to 1000 °C, the highest temperature in the present study, a weight loss of 2.3% was observed, corresponding to ~9.2% of total oxygen content. The observed high deviation from the oxygen stoichiometry in SCCN at high temperatures should be suitable for the application in ITSOFC cells, as it favours for efficient oxygen ion transport in the cathode material. High values of the oxygen nonstoichiometry at high temperatures were already observed in other strontium-rich $SrCoO_{3-\delta}$ perovskites.

The electrical conductivity of SCCN as a function of temperature is shown in Fig. 3. Generally, the undoped $SrCoO_{3-\delta}$ is a semiconductor. The co-doping of Ce^{4+} and Nb^{5+} not only improves the structure stability of the material, but also changes its conductivity. The conductivity of SCCN increases with increasing temperature to a maximum value of 516 S cm^{-1} around 300 °C. This semiconducting trend follows a thermally activated p-type small

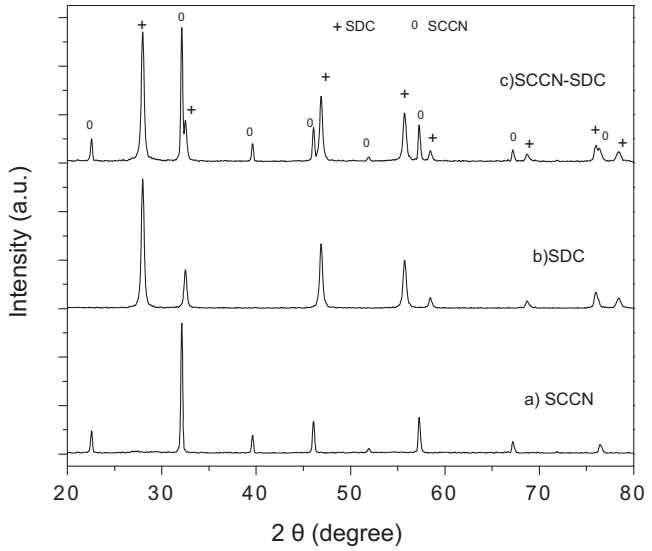

Fig. 1. X-ray diffraction patterns of the as-prepared powders: a) SCCN, b) SDC, and c) SCCN–SDC.

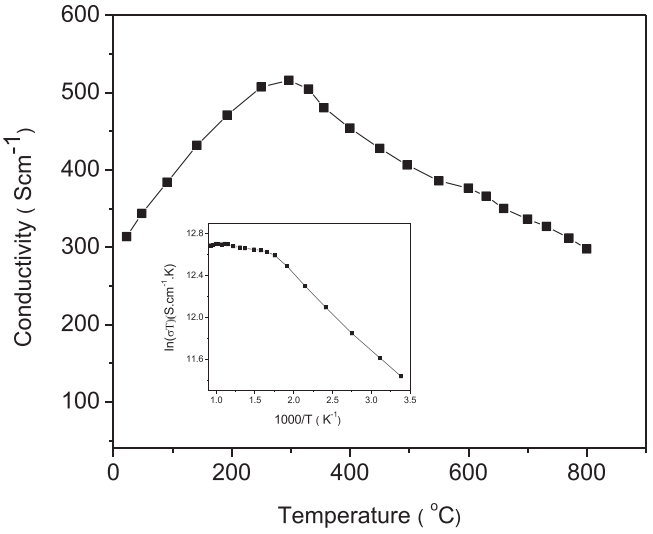

Fig. 3. Temperature dependence of the electrical conductivity of SCCN in air and the Arrhenius plots of ln(σT) vs. $1/T$ in the inset.

polaron hopping mechanism [20,27,29]. The conductivity of SCCN subsequently decreases with increasing temperature beyond 300 °C. The decrease of the conductivity is mainly associated with the loss of the lattice oxygen at elevated temperatures. This is due to the increase in the concentration of oxygen vacancies within the oxide lattice, which causes a barrier for electron hopping between the B-site cations and oxygen ions. The conduction mechanism in the thermally activated region follows Eq. (2).

$$\sigma = \frac{A}{T}\exp\left(-\frac{E_a}{kT}\right) \tag{2}$$

where, E_a is activation energy, k Boltzmann constant, T absolute temperature and A pre-exponential factor. The Arrhenius plots of ln(σT) vs. $1/T$ are shown in the inset of Fig. 3. The conductivity values of the SCCN in the temperature range of ITSOFCs are 297–516 S cm^{-1}, which are higher than the maximum conductivity of BSCF at the same temperature range [10]. It can be seen that the co-doped Ce and Nb into $SrCoO_{3-\delta}$ would break the charge balance in the material. The electrical neutrality of SCCN could be realized by both varying the valence state of the B-site ions and forming oxygen vacancies. Therefore, both oxygen vacancies and the transition of Co^{4+} to Co^{3+} lead to the increase in electron holes and the conductivity [17,18,20,27,29]. The high electrical conductivity is beneficial for improving the charge-transfer process for the ORR on the cathode.

Fig. 4 shows the typical impedance spectra of the SCCN cathode at 650 °C in air. The high-frequency intercept of the electrode impedance on the real axis is the ohmic resistance of the symmetric cell, while the difference between the low-frequency and the high-frequency intercepts on the real axis corresponds to non-ohmic resistance of electrodes, which is the area specific resistance (ASR). In general, the high-and-intermediate frequency arc (R_1) is likely associated with the charge-transfer process at the electrolyte–electrode and air–electrode interfaces, namely at the vicinity of the three-phase boundaries (TPBs). Whereas the low-frequency arc (R_2)

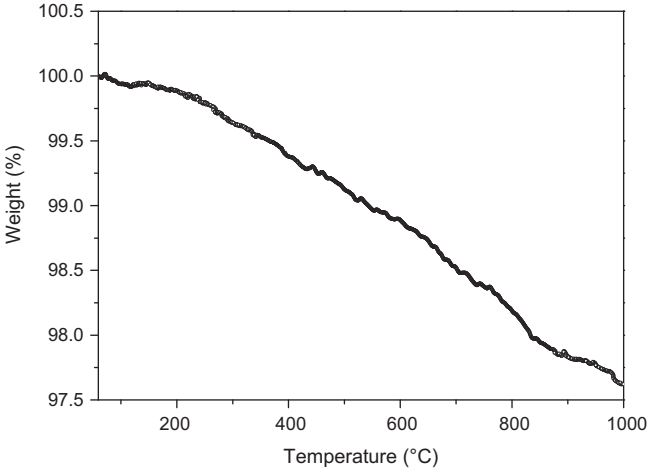

Fig. 2. TG curve of SCCN powders in air.

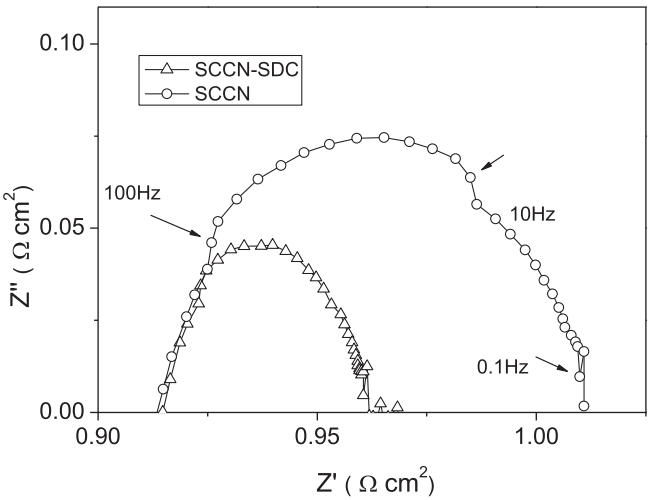

Fig. 4. Nyquist plots of the impedance of the SCCN and SCCN–SDC cathode measured at 650 °C.

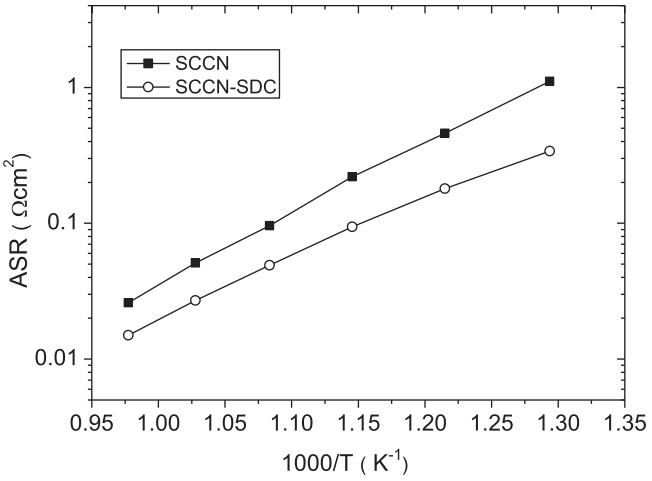

Fig. 5. The ASRs of the SCCN cathode and the SCCN–SDC cathode vs. temperature.

is caused by oxygen surface adsorption, dissociation, and oxygen ion diffusion as well as gas diffusion at the cathode surface [5,34].

Fig. 5 shows the ASRs of the SCCN cathode in air. It is clear that the ASR significantly decreases with the increasing temperature. The ASR of the SCCN cathode is 1.103, 0.461, 0.212, 0.096, 0.051, and 0.026 Ω cm^2 at 500, 550, 600, 650, 700, and 750 °C, respectively. It is worth noting that the ASR values of the SCCN cathode are higher than those of the BSCF and $SrNb_{0.1}Co_{0.9}O_3$ (SNC) cathodes at the same temperatures [10,20]. Nevertheless the structure of SCCN is more stable than those of the BSCF and SNC cathodes, due to Ce^{4+} doping on the A site and Nb^{5+} doping on the B site. From Fig. 4, one can see that R_2 of the SCCN cathode is about 0.038 Ω cm^2 and larger than R_1 (about 0.011 Ω cm^2) at 650 °C. This suggests that the cathode performance (ASR) is likely to be limited by low oxygen-ion conductivity as the lack of oxygen ion carriers in this material. To improve the electrochemical performance of the SCCN cathode, 50 wt.% SDC was added into the SCCN to form a composite cathode. This leads to the decrease in the ASR values. Besides the TEC value decreases to a value close to that of SDC. From Fig. 5, it was seen that the addition of SDC can dramatically improve the electrochemical performance of SCCN, namely decrease the ASRs.

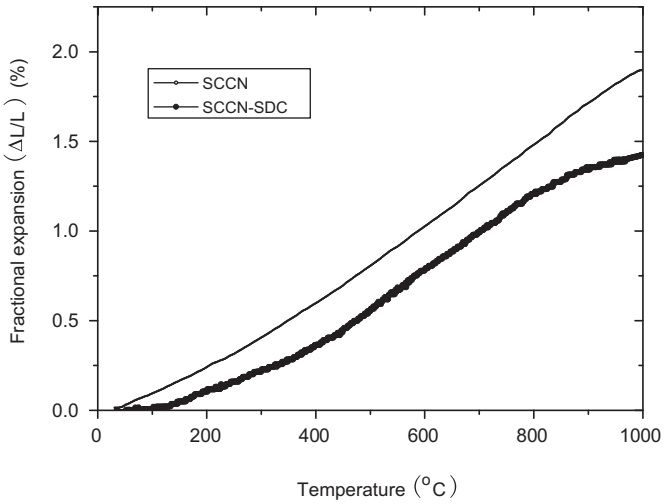

Fig. 6. Thermal expansion coefficient of SCCN and SCCN–SDC.

The ASR of the SCCN–SDC cathode was 0.094, 0.049, and 0.027 Ω cm^2 at 600, 650, and 700 °C, respectively. The addition of 50 wt.% of SDC to SCCN results in the reduction of ASR value from 0.096 to 0.049 Ω cm^2 by a factor ~2 at 650 °C. It is well-known that the electrochemical reaction at the electrodes in SOFCs is generally believed to occur at the interface among gas, electronic conductor, oxygen ion conductor, which is termed the triple-phase boundaries (TPBs). When the SCCN was mixed with SDC, it can also significantly extend the TPBs for ORR, giving rise to an enhanced performance of the composite cathode [5,33].

Large differences in TECs may induce a large internal stress during the heating and cooling processes, which negatively affects the cell operational stability. The TECs of the SCCN and SCCN–SDC composite samples are shown in Fig. 6. The plot shows a nearly linear expansion of SCCN without any abrupt changes due to structural phase transition. It has been reported that the TEC value of $SrCoO_3$ is about 20.2 × 10^{-6} K^{-1}. However, the measured TEC value of SCCN is about 18.4 × 10^{-6} K^{-1}, which is still higher than that of SDC (12.7 × 10^{-6} K^{-1}), This indicates that there is a significant thermal-expansion mismatch problem between the SCCN cathode and SDC electrolyte. When the SCCN is composited with 50 wt.% SDC, the TEC value of SCCN–SDC is about 14.3 × 10^{-6} K^{-1} as shown in Fig. 6. This result implies that a better thermal matching with SDC electrolyte can be achieved by optimizing the initial molar ratio of the two components.

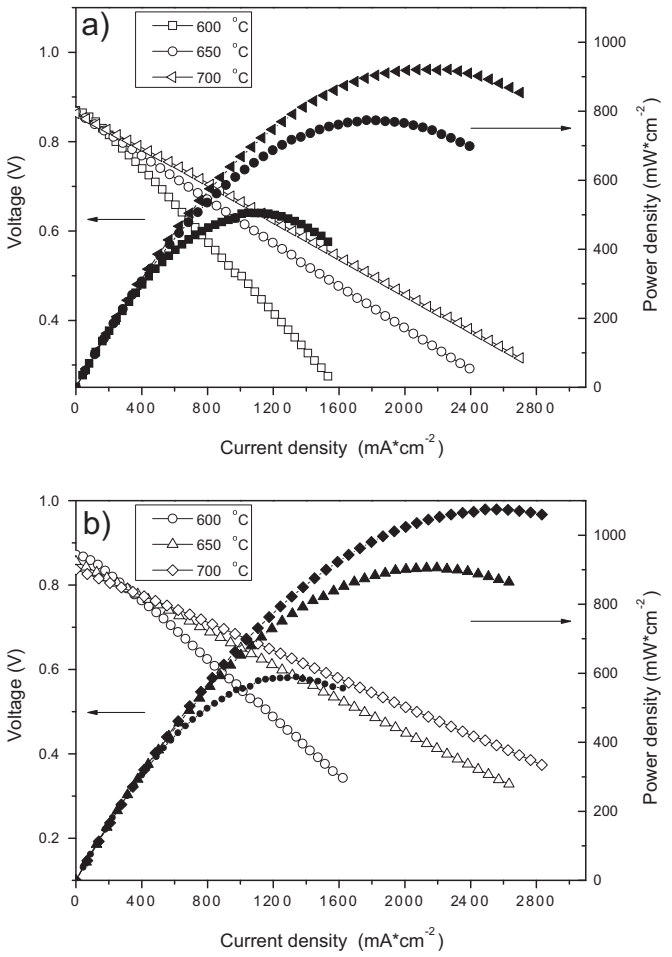

Fig. 7. *I–V* and *I–W* curves for SOFCs with a) the SCCN cathode and b) the SCCN–SDC cathode.

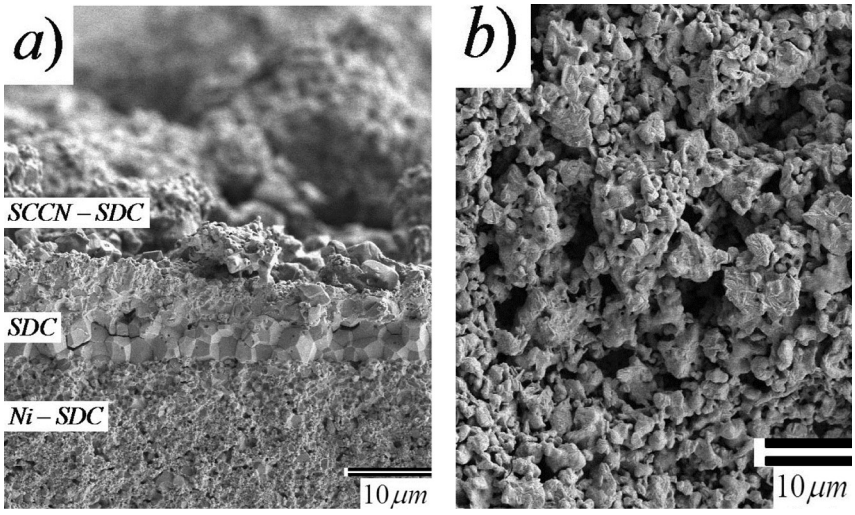

Fig. 8. SEM images a) cross-sectional of the Ni–SDC|SDC|SCCN–SDC single cell and b) the surface of the SCCN–SDC cathode.

In order to further investigate SCCN as a cathode material for ITSOFCs, the single cells were prepared with about 10 μm-thick SDC electrolyte. Fig. 7 shows the cell voltages and power densities at various temperatures. The OCV is lower than the theoretical value due to partial reduction of Ce^{4+} to Ce^{3+} at elevated temperatures, which leads to electrical conductivity in the electrolyte. One can see from Fig. 7a, the maximum power density of the cell with the SCCN cathode was found to be 505, 773, and 921 mW cm^{-2} at 600, 650, and 700 °C, respectively. Whereas the peak power densities of the cell with the SCCN–SDC cathode (shown in Fig. 7b) were as high as 589, 905, and 1074 mW cm^{-2} at 600, 650, and 700 °C, respectively. These values are comparable with those obtained from cells based on advanced cathodes operated under the same conditions such as BSCF and SNC. It should be pointed out that the performance of the fuel cell with the SCCN cathode can still be significantly improved by optimizing the microstructures of the cathode. All these results suggest that SCCN is a very promising cathode candidate for ITSOFCs with SDC electrolytes.

Fig. 8(a) shows the typical cross-section SEM image of the tested cell Ni–SDC|SDC|SCCN–SDC. The SDC membrane and SCCN–SDC cathode layer are about 10 and 40 μm in thickness, respectively. One can clearly see that SCCN–SDC cathode and Ni–SDC anode still adheres to the SDC electrolyte quite well after test. The results support the absence of a significant phase reaction between SCCN–SDC and SDC during the high-temperature fabrication. Shown in Fig. 8(b) is the surface SEM image of the SCCN–SDC cathode sintered at 1000 °C for 1 h. The SEM image shows that the cathode contains regular-shaped particles with about 1–3 μm in size. The porosity of the SCCN–SDC cathode is about 36%. The cathode particles connect with each other forming a porously continuous network microstructure.

4. Conclusions

A cobalt-containing perovskite oxide $Sr_{0.9}Ce_{0.1}Co_{0.9}Nb_{0.1}O_{3-\delta}$ (SCCN) has been investigated as a cathode material for ITSOFCs. The SCCN cathode was chemically compatible with SDC electrolyte at temperatures up to 1000 °C. The electrical conductivity of SCCN reaches high values of 297–516 S cm^{-1} in air in the temperature range of RT–800 °C. Doping of highly charged Ce^{4+} and Nb^{5+} ions successfully stabilizes the perovskite structure and avoids order–disorder phase transition. The ASR of the SCCN–SDC cathode was 0.094, 0.049, and 0.027 Ω cm^2 at 600, 650, and 700 °C, respectively. The maximum power density of 1074 mW cm^{-2} was obtained at 700 °C for the single cell Ni–SDC|SDC|SCCN–SDC. The relatively low TEC of SCCN–SDC is 14.3 × 10^{-6} K^{-1} in air. All these results demonstrate that SCCN is a very promising cathode material for ITSOFCs.

Acknowledgements

The authors gratefully acknowledge financial support from National Natural Science Foundation of China (grant no. 11074001), Anhui Provincial Natural Science Foundation of China (grant no. 1308085MB19), and Scientific Research Foundation of Education Ministry of Anhui Province of China (grant no. KJ2013A008).

References

[1] N.Q. Minh, J. Am. Ceram. Soc. 76 (1995) 563–588.
[2] B.C.H. Steele, A. Heinzel, Nature 414 (2001) 345–352.
[3] J. Fleig, Annu. Rev. Mater. Res. 33 (2003) 361–382.
[4] A.J. Jacobson, Chem. Mater. 22 (2010) 660–674.
[5] S.B. Adler, Chem. Rev. 104 (2004) 4791–4843.
[6] E.D. Wachsman, K.T. Lee, Science 334 (2011) 935–939.
[7] E. Ivers-Tiffee, A. Weber, D. Herbstritt, J. Eur. Ceram. Soc. 21 (2001) 1805–1811.
[8] E.V. Tsipis, V.V. Kharton, J. Solid State Electrochem. 12 (2008) 1039–1060.
[9] H.Y. Tu, Y. Takeda, N. Imanishi, O. Yamamoto, Solid State Ionics 117 (1999) 277–281.
[10] Z.P. Shao, S.M. Haile, Nature 431 (2004) 170–173.
[11] E.P. Murray, M.J. Sever, S.A. Barnett, Solid State Ionics 148 (2002) 27–34.
[12] D.H. Lee, I.Y. Jung, S.O. Lee, S.H. Hyun, J.H. Jang, J.H. Moon, Int. J. Hydrogen Energy 36 (2011) 6875–6881.
[13] J.W. Stevenson, T.R. Armstrong, R.D. Carneim, L.R. Pederson, W.J. Weber, J. Electrochem. Soc. 143 (1996) 2722–2729.
[14] A. Aguadero, C. Calle, J.A. Alonso, M.J. Escudero, M.T. Fernandez-Dıaz, L. Daza, Chem. Mater. 19 (2007) 437–444.
[15] A. Aguadero, D. Perez-Coll, J.A. Alonso, S.J. Skinner, J. Kilner, Chem. Mater. 24 (2012) 2655–2663.
[16] Z.Q. Deng, J.P. Smit, H.J. Niu, G. Evans, M.R. Li, Z.L. Xu, J.B. Claridge, M.J. Rosseinsky, Chem. Mater. 21 (2009) 5154–5162.
[17] P.Y. Zeng, Z.P. Shao, S.M. Liu, Z.P. Xu, Sep. Purif. Technol. 67 (2009) 304–311.
[18] K. Zhang, R. Ran, L. Ge, Z.P. Shao, W.Q. Jin, N.P. Xu, J. Membr. Sci. 323 (2008) 436–443.
[19] T. Nagai, W. Ito, T. Sakon, Solid State Ionics 177 (2007) 3433–3444.
[20] W. Zhou, W.Q. Jin, Z.H. Zhu, Z.P. Shao, Int. J. Hydrogen Energy 35 (2010) 1356–1366.
[21] L.L. Zhang, W. Long, F.J. Jin, T.M. He, Int. J. Hydrogen Energy 38 (2013) 7947–7956.
[22] S.Y. Yoo, T.H. Lim, J.Y. Shin, G. Kim, J. Power Sources 226 (2013) 1–7.
[23] Y. Lin, R. Ran, D.J. Chen, Z.P. Shao, J. Power Sources 195 (2010) 4700–4703.
[24] M.T. Colomer, B.C.H. Steele, J.A. Kilner, Solid State Ionics 147 (2002) 41–48.
[25] N.E. Trofimenko, H. Ullmann, J. Eur. Ceram. Soc. 20 (2000) 1241–1250.
[26] H.T. Gu, H. Chen, L. Gao, Y.F. Zheng, X.F. Zhu, L.C. Guo, Int. J. Hydrogen Energy 33 (2008) 4681–4688.

[27] N.E. Trofimenko, J. Paulsen, H. Ullmann, R. Miiller, Solid State Ionics 100 (1997) 183–191.
[28] F. Deganelloa, L.F. Liott, A. Longo, M.P. Casaletto, M. Scopelliti, J. Solid State Chem. 179 (2006) 3406–3419.
[29] Q.T. Wei, R.S. Guo, F.H. Wang, H.L. Li, J. Mater. Sci. 40 (2005) 1317–1319.
[30] W. Yang, T. Hong, S. Li, Z.H. Ma, C.W. Sun, C.R. Xia, L.Q. Chen, ACS Appl. Mater. Interfaces 5 (2013) 1143–1148.
[31] S.W. Zha, C.R. Xia, G.Y. Meng, J. Power Sources 115 (2003) 44–48.
[32] H. Moon, S.D. Kim, S.H. Hyun, H.S. Kim, Int. J. Hydrogen Energy 33 (2008) 2826–2833.
[33] A. Aguadero, C. Calle, J.A. Alonso, M.J. Escudero, M.T. Fernandez-Diaz, L. Daza, Chem. Mater. 19 (2007) 6437–6444.
[34] M.A. Haider, S. McIntosh, J. Electrochem. Soc. 156 (2009) B1369–B1375.